Available online at www.sciencedirect.com
ScienceDirect
Physics Letters A 366 (2007) 528–533
PHYSICS LETTERS A
www.elsevier.com/locate/pla

Weak-light gap solitons in a resonant three-level system

Jing Wang, Chao Hang, Guoxiang Huang *

Department of Physics, East China Normal University, Shanghai 200062, China

Received 24 January 2007; accepted 9 February 2007

Available online 23 March 2007

Communicated by V.M. Agranovich

Abstract

We propose a scheme of generating optical gap solitons in a resonant three-level atomic system via electromagnetically induced transparency. We demonstrate, both analytically and numerically, that by means of a strong standing-wave control field the soliton with oscillating frequency within the band gap of a weak probe field can appear. Different from conventional passive optical media, the gap soliton in such highly resonant system can be created with very weak light intensity and can be manipulated in a controllable way.

PACS: 42.65.Tg; 05.45.Yv; 42.50.Gy

1. Introduction

In the past decades, considerable research activities have focused on the study of optical solitons due to their important applications in optical information processing and transmission [1,2]. Up to now, most optical solitons are produced in passive optical media such as glass-based optical fibers, in which far-off resonance excitation schemes are generally employed in order to avoid unmanageable optical attenuation and distortion. However, due to the lack of distinctive energy levels, the nonlinear effect in such passive optical media is very weak, and hence a very high light intensity is required to form a soliton. In addition, the lack of distinctive energy levels and transition selection rules also makes an active control of such optical soliton difficult.

In recent years, much attention has been paid to the investigation on the optical property of an active optical medium via electromagnetically induced transparency (EIT) [3,4], in which an on-resonance excitation scheme is employed. Due to the quantum interference effect induced by a control field, the wave propagation of a weak probe field in such medium display many striking features [3,4], including a large suppression of optical absorption and a significant reduction of group velocity. Based on these interesting features, in recent works [5–9] it has been shown that a new type of optical solitons, called ultraslow optical solitons, can form in resonant three-level and four-level media. Such study has opened a new research direction on nonlinear wave propagation in coherent multi-level media.

Recently, the coherent manipulation of light pulses via dynamically controlled photonic band gap in EIT media has been investigated both theoretically and experimentally [10–14]. It is widely expected that a further exploration in this direction may offer new tools of photonic state manipulation and quantum information processing at low-light level [14]. In the present work, we propose a scheme for the formation of an optical gap soliton in a resonant three-level atomic system via EIT technique. Different from previous studies in Refs. [5–9], the control field used here is an optical standing-wave, which induces a periodic variation of linear refractive index. We shall demonstrate that the oscillating frequency of the soliton found by us is within the forbidden gap of frequency spectrum of the probe field. Notice that gap solitons in passive optical media have been studied intensively [15,16] since the pioneer work of Chen and Mills [17]. Because our system is an active medium, the gap soliton in such system can be

* Corresponding author.
E-mail address: gxhuang@phy.ecnu.edu.cn (G. Huang).

0375-9601/$ – see front matter
doi:10.1016/j.physleta.2007.02.103

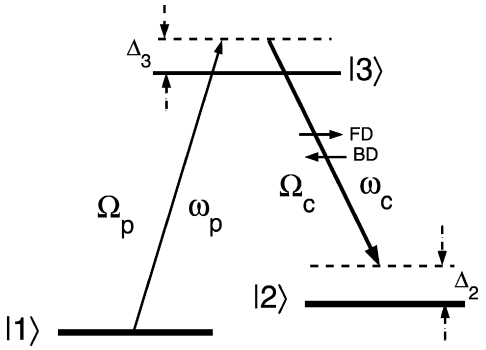

Fig. 1. Lifetime-broadened three-level atomic system interacting with a strong control field (with angular frequency ω_c and Rabi frequency $2\Omega_c$) and a weak probe field (with angular frequency ω_p and Rabi frequency $2\Omega_p$). FD and BD represent respectively forward and backward propagating components of the control field. Δ_3 and Δ_2 are one-photon and two-photon detunings, respectively.

generated with very weak light intensity and also can be manipulated in a controllable way. Because of their robust nature, such optical solitons may become promising candidates of well-characterized, distortion-free optical pulses and hence have potential technological applications in optical and telecommunication engineering.

The Letter is arranged as follows. The next section gives a simple description of our three-level model. In Section 3 we derive a set of coupled nonlinear envelope equations by using a method of multiple-scales and discuss their soliton solutions. To test our analytical calculation, in Section 4 we present a numerical study on the gap soliton starting from Maxwell–Schrödinger equations. Finally, the last section contains a summary and conclusion of our main results.

2. The model

The physical model we consider is a lifetime broadened three-level atomic system interacting with a weak pulsed probe field of center angular frequency ω_p (coupling $|1\rangle \to |3\rangle$ transition) and a strong continuous-wave control field of center angular frequency ω_c (coupling $|3\rangle \to |2\rangle$ transition), respectively (see Fig. 1). In particular, the control field is an optical standing wave consisting of forward (FD) and backward (BD) propagating parts in order to provide the background periodic linear refractive index for the probe field. The electric-field vector of the system can be written as $\mathbf{E} = \mathbf{e}_p\{\mathcal{E}_+ \exp[i(k_p z - \omega_p t)] + \mathcal{E}_- \exp[-i(k_p z + \omega_p t)]\} + 4\mathbf{e}_c\mathcal{E}_c \cos(k_c z)\cos(\omega_c t)$, where Ω_c ($\Omega_\pm$) is a real constant (complex function of z and t), k_j and $\mathbf{e}_j$ are wavevectors and polarization directions of the probe ($j = p$) and control ($j = c$) fields, respectively. In interaction picture, the interaction Hamiltonian can be expressed in the Hilbert space spanned by the bare states $|j\rangle$ (with eigenenergy E_j, $j = 1, 2, 3$) under a rotating-wave approximation:

$$\hat{H}_1' = -\hbar\big[\big(\Omega_+ e^{ik_p z} + \Omega_- e^{-ik_p z}\big)|3\rangle\langle 1| + 2\Omega_c \cos(k_c z)|3\rangle\langle 2| + \text{H.c.}\big], \tag{1}$$

where $\Omega_+ = [(\mathbf{e}_p \cdot \mathbf{p}_{31})\mathcal{E}_+]/\hbar$ and $\Omega_- = [(\mathbf{e}_p \cdot \mathbf{p}_{31})\mathcal{E}_-]/\hbar$ are respectively half Rabi frequencies of the probe field for the FD and BD components, $\Omega_c = [(\mathbf{e}_c \cdot \mathbf{p}_{32})\mathcal{E}_c]/\hbar$ is the half Rabi frequency of the control field, and $\mathbf{p}_{ij}$ is the electric dipole matrix element associated with the transition from $|i\rangle$ to $|j\rangle$.

The Schrödinger equation governing the motion of atomic state amplitudes A_j ($j = 1, 2, 3$) in the interaction picture reads

$$\left(i\frac{\partial}{\partial t} + d_2\right)A_2 + 2A_3\Omega_c \cos(k_c z) = 0, \tag{2a}$$

$$\left(i\frac{\partial}{\partial t} + d_3\right)A_3 + A_1\big[\Omega_+ e^{ik_p z} + \Omega_- e^{-ik_p z}\big] + 2A_2\Omega_c \cos(k_c z) = 0, \tag{2b}$$

with $\sum_{j=1}^{3}|A_j|^2 = 1$. In above equations $d_j = \Delta_j + i\gamma_j$ ($j = 1, 2$) with $\Delta_3 = \omega_p - (E_3 - E_1)/\hbar$ and $\Delta_2 = \omega_p - \omega_c - (E_2 - E_1)/\hbar$ being one- and two-photon detunings, respectively. The parameter γ_j denotes the decay rate of the state $|j\rangle$.

Under a rotating-wave approximation, the Maxwell equation controlling the time evolution of the electric field $\mathbf{E}$ is reduced to

$$\left(\frac{\partial^2}{\partial z^2} - \frac{1}{c^2}\frac{\partial^2}{\partial t^2}\right)\big[D(z)e^{-i\omega_p t}\big] = \kappa_0\frac{\partial^2}{\partial t^2}\big(A_3 A_1^* e^{-i\omega_p t}\big), \tag{3}$$

where $D(z) = \Omega_+ e^{ik_p z} + \Omega_- e^{-ik_p z}$, and $\kappa_0 = N_a|\mathbf{p}_{31}|^2/(\hbar\varepsilon_0 c^2)$ is a coupling constant with N_a being atomic density of the system. Eqs. (2) and (3) are our model system employed in the following calculations.

3. Asymptotic expansion and coupled mode equations

As in usual EIT case we assume that the probe field is very weak in comparison with the control field, i.e. $|\Omega_\pm| \ll \Omega_c$. In addition, we assume also that the pulse length of the probe field is large enough so that an adiabatic approximation for Eqs. (2)

can apply. As a result we have $A_j = f_j(z)A_1$ and $|A_1|^2 = [1 + (|f_1|^2 + |f_2|^2)]^{-1}$, with $f_j(z) = g_j(z)D(z)$ $(j = 2, 3)$. Here $g_2(z) = -2\Omega_c \cos(k_c z)/[4\Omega_c^2 \cos^2(k_c z) - d_2 d_3]$ and $g_3(z) = d_2/[4\Omega_c^2 \cos^2(k_c z) - d_2 d_3]$. Thus Eq. (3) can be rewritten as

$$\left(\frac{\partial^2}{\partial z^2} - \frac{1}{c^2}\frac{\partial^2}{\partial t^2}\right)\left[D(z)e^{-i\omega_p t}\right] = \kappa_0 \frac{\partial^2}{\partial t^2}\left\{\frac{g_3 D(z)}{1 + (|g_2|^2 + |g_3|)^2|D(z)|^2} e^{-i\omega_p t}\right\}. \tag{4}$$

It is a nonlinear wave equation describing the spatio-temporal evolution of the probe field. Notice that, in the case of very small $|\Omega_\pm|$, Eq. (4) becomes a linear one with a periodic coefficient in z. So its eigenspectrum displays forbidden gap.

We are interested in possible soliton formation in the system and hence the nonlinear effect in Eq. (4) must be take into account. For simplicity, we consider the case of large detuning, i.e. $4\Omega_c^2/d_2 d_3 = \epsilon^2 A_0$ ($\epsilon \ll 1$, $|A_0| \approx \mathcal{O}(1)$). Then one has $g_2 = \epsilon\sqrt{A_0/(d_2 d_3)}\cos(k_c z)[1 + \epsilon^2 A_0 \cos^2(k_c z) + \mathrm{O}(\epsilon^4)]$ and $g_3 = -(1/d_3)[1 + \epsilon^2 A_0 \cos^2(k_c z) + \mathrm{O}(\epsilon^4)]$. We employ the powerful method of multiple-scales [18] to derive the nonlinear coupled envelope equations for the FD and BD components of the probe field. We start by making the following asymptotic expansion $\Omega_\pm = \sum_{l=1}^{\infty} \epsilon^l \Omega_\pm^{(l)}$. To obtain a divergence-free solution in high-order approximations, all quantities on the right-hand side of the asymptotic expansion must be considered as functions of the multi-scale variables $z_l = \epsilon^l z$ $(l = 0, 2)$ and $t_l = \epsilon^l t$ $(l = 0, 2)$. Substituting such expansion into Eq. (4), we obtain a chain of linear, but inhomogeneous equations on $\Omega_\pm^{(l)}$, which can be solved order by order.

In the leading order, i.e. exact to $\mathrm{O}(\epsilon)$, the Rabi frequencies of the forward and backward propagating components of the probe field fulfill the equation

$$\left(\frac{\omega_p^2}{c^2} - k_p^2\right)\Omega_\pm^{(1)} = \frac{\kappa_0 \omega_p^2}{d_3}\Omega_\pm^{(1)}, \tag{5}$$

which gives $k_p = \omega_p n_p/c$ with the linear refraction index $n_p = \sqrt{1 - N_a|\mathbf{p}_{31}|^2/(\hbar\varepsilon_0 d_3)}$. We see that under the condition $|\Delta_3| \gg \gamma_3$, one gets $n_p > 1$ when $\Delta_3 < 0$ and $n_p < 1$ when $\Delta_3 > 0$.

In the next order, i.e. exact to $\mathrm{O}(\epsilon^3)$, we obtain a set of closed coupled mode equations governing the evolution of $\Omega_\pm^{(1)}$. They can be written as the form

$$i\left(\frac{\partial}{\partial z} + \frac{n_p}{c}\frac{\partial}{\partial t}\right)u = \frac{\kappa_0\omega_p^2}{2d_3 k_p}\left[\frac{B_0}{2}\left(u + \frac{1}{2}ve^{2i\Delta k z}\right) - \frac{1}{|d_3|^2}\left(|u|^2 + 2|v|^2\right)u\right], \tag{6a}$$

$$i\left(-\frac{\partial}{\partial z} + \frac{n_p}{c}\frac{\partial}{\partial t}\right)v = \frac{\kappa_0\omega_p^2}{2d_3 k_p}\left[\frac{B_0}{2}\left(v + \frac{1}{2}ue^{-2i\Delta k z}\right) - \frac{1}{|d_3|^2}\left(|v|^2 + 2|u|^2\right)v\right], \tag{6b}$$

when returning to original variables. Note that when obtaining Eq. (6) we have defined $B_0 = 4\Omega_c^2/(d_2 d_3)$ and used the notations $u = \epsilon\Omega_+^{(1)}$ and $v = \epsilon\Omega_-^{(1)}$. In particular, we have assumed Bragg resonance condition $k_p = k_c + \Delta k$ with $\Delta k \approx \mathcal{O}(\epsilon)$, where a gap of the linear spectrum is open, as shown below.

By the transformation $u = U\exp[i(\Delta k z - c_f t)]$ and $v = V\exp[-i(\Delta k z + c_f t)]$ with $c_f = c\kappa_0\omega_p^2 B_0/4n_p d_3 k_p$, the exponential factors in Eqs. (6) can be removed. Then we have

$$i\left(\frac{\partial}{\partial z} + \frac{n_p}{c}\frac{\partial}{\partial t}\right)U = \Delta k U + \kappa V - \Gamma\left(|U|^2 + 2|V|^2\right)U, \tag{7a}$$

$$i\left(-\frac{\partial}{\partial z} + \frac{n_p}{c}\frac{\partial}{\partial t}\right)V = \Delta k V + \kappa U - \Gamma\left(|V|^2 + 2|U|^2\right)V, \tag{7b}$$

where $\Gamma = \kappa_0\omega_p^2/(2d_3|d_3|^2 k_p)$ is the nonlinear coefficient characterizing the strength of self-phase as well as cross-phase modulations, and $\kappa = \kappa_0\omega_p^2 B_0/(8d_3 k_p)$ is the constant describing the coupling strength of linear interaction between the FD and BD components of the probe field.

In linear level, Eqs. (7) admits the plane wave solution $(U, V) = (U_0, V_0)\exp[i(Kz - \omega t)]$. The linear dispersion relation displays two branches

$$\omega = \omega_\pm = \frac{c}{n_p}\left[\Delta k \pm \sqrt{\kappa^2 + K^2}\right], \tag{8}$$

which has been show in Fig. 2 for $\Delta_j \gg \gamma_j$ $(j = 2, 3)$. We see that there is a frequency gap between the two dispersion branches. The gap width is given by

$$\Delta\omega_{\mathrm{gap}} = \omega_+|_{K=0} - \omega_-|_{K=0} = \frac{2c\kappa}{n_p}. \tag{9}$$

Notice that since $\kappa \sim B_0 \sim \Omega_c^2$, the gap width can be changed very easily by just tuning the amplitude of the control field.

Now we turn to consider the soliton solution of the full nonlinear equations (7a) and (7b). In general, these equations admit no soliton solution because their coefficients are complex. However, due to the EIT effect induced by the strong control field, it can be

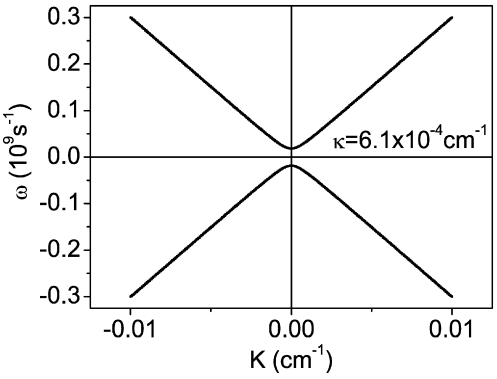

Fig. 2. Linear dispersion relation of the couple-mode equations with wavevector K and frequency ω. The coupling constant is chosen as $\kappa = 6.1 \times 10^{-4}$ cm^{-1}.

shown that the imaginary parts of these coefficients are much less than their real parts (see a practical numerical example given in the next section) and hence can be taken as a small perturbation. When neglecting such perturbation,[1] Eqs. (7a) and (7b) admit the following coupled soliton solution [19]

$$U = \alpha F_+(z,t)e^{i\eta(\theta)}, \tag{10a}$$

$$V = \alpha F_-(z,t)e^{i\eta(\theta)}, \tag{10b}$$

$$e^{i\eta(\theta)} = \left(-\frac{e^{2\theta} + e^{\mp i\delta_0}}{e^{2\theta} + e^{\pm i\delta_0}}\right)^{2v_0/(3-v_0^2)}, \tag{10c}$$

where $\theta = \gamma_0\kappa_r \sin\delta_0(z - v_0 ct/n_{pr})$ and $\psi = \gamma_0\kappa_r \cos\delta_0(v_0 z - ct/n_{pr})$. $F_\pm$ are the coupled soliton solution of the massive Thirring model [20], having the form

$$F_+ = \pm\left(\mp\frac{\kappa_r}{2\Gamma_r}\right)^{1/2}\frac{1}{\rho_0}\sin\delta_0 e^{\pm i\psi}\,\mathrm{sech}\left(\theta \mp \frac{i\delta_0}{2}\right), \tag{11a}$$

$$F_- = -\left(\mp\frac{\kappa_r}{2\Gamma_r}\right)^{1/2}\rho_0\sin\delta_0 e^{\pm i\psi}\,\mathrm{sech}\left(\theta \pm \frac{i\delta_0}{2}\right). \tag{11b}$$

In Eqs. (10) and (11) we have defined the real parameters $\alpha_0 = \sqrt{(2-2v_0^2)/(3-v_0^2)}$ and $\gamma_0 = 1/\sqrt{1-v_0^2}$ with $v_0 = (1-\rho_0^4)/(1+\rho_0^4)$. ρ_0 and δ_0 are two free parameters (ρ_0 is dimensionless and $0 < \delta_0 < \pi$) determining the propagating velocity and temporal width of the soliton, respectively. The quantities κ_r, n_{pr}, Γ_r are the real parts of κ, n_p, and Γ, respectively. The signs in Eqs. (11) are determined by those of the linear and nonlinear coupling coefficients. With such coupled soliton solution the Rabi frequency of the probe field reads $D(z) \equiv \Omega_p(z,t) = \Omega_+ e^{ik_p z} + \Omega_- e^{-ik_p z} = U\exp\{i[(k_p + \Delta k)z - c_f t]\} + V\exp\{-i[(k_p + \Delta k)z + c_f t]\}$, with U and V given by Eqs. (10a) and (10b).

4. Numerical simulation

We consider that the control and probe fields propagate in a gas cell filled with cold alkali atoms (e.g. ^{87}Rb or ^{23}Na) of density $N_a = 1.0 \sim 1.6 \times 10^{10}$ cm^{-3}. The decay rates (detunings) of the states $|2\rangle$ and $|3\rangle$ are $\gamma_2 = 1.0 \times 10^4$ s^{-1} ($\Delta_2 = 1.0 \times 10^8$ s^{-1}) and $\gamma_3 = 6.0 \times 10^6$ s^{-1} ($\Delta_3 = -1.0 \times 10^9$ s^{-1}), respectively. With these realistic parameters, we obtain $\kappa = -(6.09 + 0.073i) \times 10^{-4}$ cm^{-1}, $n_p = 1.0 + 4.6 \times 10^{-16}i$, and $\Gamma = -(6.09 + 0.036i) \times 10^{-7}$ cm^{-1}. We see that the imaginary parts of these parameters are indeed much smaller than their corresponding real parts. The physical reason of such small imaginary parts is due to the quantum destructive interference effect induced by the control field (i.e. EIT effect). It is easy to show that soliton solution obtained in the last section corresponds to $K = K_s \equiv \gamma_r\kappa_r \cos\delta_0 v_0$, with the oscillating frequency $\omega_s = \gamma_r\kappa_r \cos\delta_0 c/n_{pr}$. With the choice of our parameters, we get $|K_s| \simeq 0$ and

$$|\omega_s| = 0.49|\Delta\omega_{\mathrm{gap}}|. \tag{12}$$

Consequently, the oscillating frequency of the soliton falls in the forbidden gap and hence it is a gap soliton.

With this result one can easily calculate the maximum mean peak power of the gap soliton, which reads $\bar{P}_{\max} = 9.01 \times 10^{-3}$ mW. This is drastically different from the conventional soliton generation technique using fibers or waveguides where picosecond or femtosecond laser pulses are needed to reach very high peak power to bring out the nonlinear effect required for soliton formation.

[1] The perturbation contributed by the imaginary parts in the coefficients of Eqs. (7a) and (7b) will be considered by numerical simulation presented in Section 4.

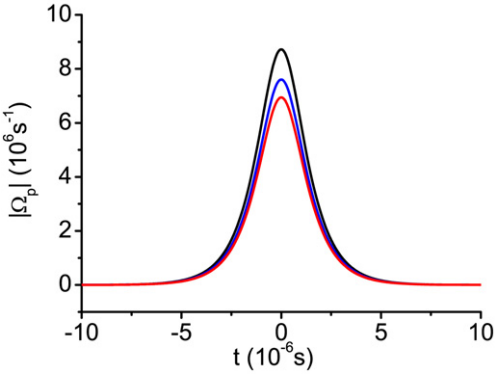

Fig. 3. The evolution of a gap soliton with the parameters $\rho = 0.90$ and $\delta = \pi/13$. The Rabi frequency of the control field and the atomic density are chosen as $\Omega_c = 1.0 \times 10^7\ \mathrm{s}^{-1}$ and $N_a = 1.6 \times 10^{10}\ \mathrm{cm}^{-3}$. The black line denotes the initial soliton probe pulse, while the blue and red lines indicate its evolution after propagating for 3.0 cm and 5.0 cm, respectively. (For interpretation of the references to colour in this figure legend, the reader is referred to the web version of this Letter.)

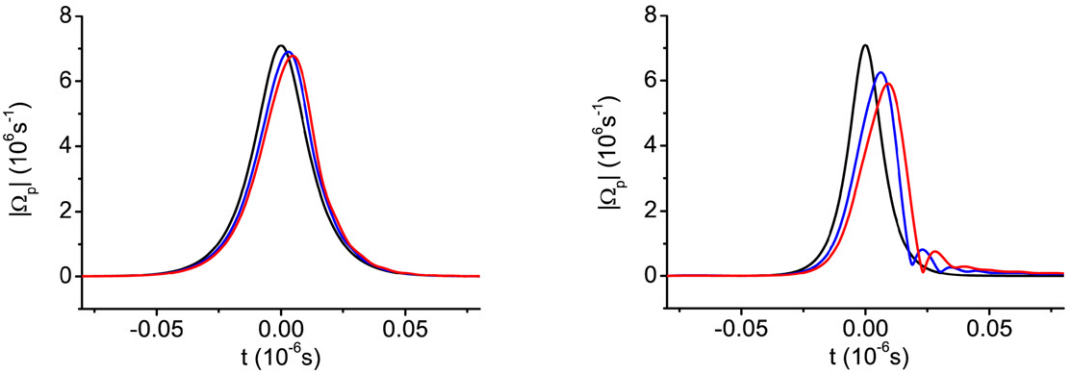

Fig. 4. The evolution of the gap soliton for two set of system parameters. Panel (a): $\rho = 0.2$, $\delta = \pi/4.0$, and $N_a = 1.0 \times 10^{10}\ \mathrm{cm}^{-3}$. Panel (b): $\rho = 0.2$, $\delta = \pi/4.0$, and $N_a = 1.6 \times 10^{10}\ \mathrm{cm}^{-3}$. In the figure the black line represents the initial soliton, and the blue line and red line are the results after the soliton propagates $z = 3.0$ cm and $z = 5.0$ cm, respectively. (For interpretation of the references to colour in this figure legend, the reader is referred to the web version of this Letter.)

In order to test the stability of the soliton solution given above, we present a numerical simulation starting directly from the Maxwell–Schrödinger equations (2) and (3) by taking the analytical result (10) and (11) as an initial condition. In Fig. 3 we have shown the evolution of an initial gap soliton, by using the parameters $\rho_0 = 0.9$, $\delta_0 = \pi/13$, $\Omega_c = 1.0 \times 10^7\ \mathrm{s}^{-1}$ and $N_a = 1.6 \times 10^{10}\ \mathrm{cm}^{-3}$. The black line indicates the initial soliton probe pulse while the blue and red lines indicate its evolution when propagating for 3.0 cm and 5.0 cm, respectively. We see that the soliton keeps its shape after propagating for a long distance without obvious deformation. Although the EIT effect suppress largely the absorption of the probe field, the absorption is, however, not zero and hence a small damping of the soliton amplitude occurs.

Shown in Fig. 4 is the soliton evolution with smaller pulse length, i.e. with smaller ρ_0. In Fig. 4(a) we choose the system parameters as $\rho_0 = 0.2$, $\delta_0 = \pi/4.0$, $\Omega_c = 1.0 \times 10^7\ \mathrm{s}^{-1}$ and $N_a = 1.0 \times 10^{10}\ \mathrm{cm}^{-3}$. We see that the soliton in this case is still fairly stable and has smaller damping in comparison with the soliton in Fig. 3. Decreasing the pulse length further, we expect high-order dispersion effect will take a significant role. This is just the case found in our numerical simulation. In Fig. 4(b) we have plotted the soliton evolution by increasing the atomic density up to $N_a = 1.6 \times 10^{10}\ \mathrm{cm}^{-3}$ for narrowing the initial pulse. We see that an obvious deformation of the soliton with a decreasing of its amplitude and a radiation of some "phonons" in its tail occurs.

5. Conclusion

We have proposed a scheme for creating an optical gap soliton in a resonant three-level atomic system via electromagnetically induced transparency. By means of the method of multiple scales, we have derived a set of coupled mode equations that govern the evolution of the forward and backward components of the probe field. The coupled soliton solution has been discussed and their stability has been tested by using a numerical simulation. We have demonstrated that by manipulating system parameters the oscillating frequency of the soliton can be indeed within the band gap of a weak probe field and hence gap soliton can appear in such highly-resonant physical system. Different from conventional passive optical media, the gap soliton found here can be created with very weak light intensity and can be manipulated in a controllable way. Because the gap solitons found here are well-characterized,

distortion-free nonlinear optical pulses, they may have promising technological applications in optical and telecommunication engineering.

Acknowledgements

The work was supported by the Key Development Program for Basic Research of China under Grant Nos. 2005CB724508 and 2006CB921104, NSF-China under Grant Nos. 10434060, 90403008 and 10674060, and by the PhD Program Scholarship Fund of ECNU 2006.

References

[1] G.P. Agrawal, Nonlinear Fiber Optics, third ed., Academic Press, New York, 2001.
[2] A. Hasegawa, M. Matsumoto, Optical Solitons in Fibers, Springer, Berlin, 2003.
[3] S.E. Harris, Phys. Today 50 (7) (1997) 36.
[4] M. Fleischhauer, et al., Rev. Mod. Phys. 77 (2005) 633, and references therein.
[5] Y. Wu, L. Deng, Phys. Rev. Lett. 93 (2004) 143904;
Y. Wu, L. Deng, Opt. Lett. 29 (2004) 2064;
Y. Wu, Phys. Rev. A 71 (2005) 053820.
[6] G. Huang, et al., Phys. Rev. E 72 (2005) 016617;
G. Huang, et al., Phys. Rev. E 73 (2006) 056606.
[7] L. Deng, et al., Phys. Rev. E 72 (2005) 055601(R).
[8] T. Hong, Phys. Rev. Lett. 90 (2003) 183901.
[9] C. Hang, et al., Phys. Rev. E 73 (2006) 036607;
C. Hang, et al., Phys. Rev. E 74 (2006) 046601.
[10] A. André, M.D. Lukin, Phys. Rev. Lett. 89 (2002) 143602.
[11] A. André, et al., Phys. Rev. Lett. 94 (2005) 063902.
[12] X.M. Su, B.S. Ham, Phys. Rev. A 71 (2005) 013821;
W. Jiang, et al., quant-ph/0511210.
[13] F.E. Zimmer, et al., quant-ph/0602197.
[14] M. Bajcsy, et al., Nature 426 (2003) 638.
[15] C.M. de Sterke, J.E. Sipe, in: Prog. Opt., vol. XXXIII, 1994, p. 203.
[16] R.E. Slusher, B.J. Eggleton, Nonlinear Photonic Crystals, Springer, Berlin, 2003, and references therein.
[17] W. Chen, D.L. Mills, Phys. Rev. Lett. 58 (1987) 160;
W. Chen, L.D. Mills, Phys. Rev. B 36 (1987) 6269.
[18] A. Jeffrey, T. Kawahara, Asymptotic Methods in Nonlinear Wave Theory, Pitman, London, 1982.
[19] A.B. Aceves, S. Wabnitz, Phys. Lett. A 141 (1989) 37.
[20] D.J. Kaup, A.C. Newell, Lett. Nuovo Cimento 20 (1977) 325.